Article

Rational design and synthesis of methyl-#-D-galactomalonyl phenyl esters as potent galectin-8N antagonists

Brijesh Patel, Chandan Kishor, Todd A. Houston, Hadaz Shatz-Azoulay, Yehiel Zick, Yaron Vinik, and Helen Blanchard

J. Med. Chem., **Just Accepted Manuscript** • DOI: 10.1021/acs.jmedchem.0c00602 • Publication Date (Web): 18 Aug 2020

Rational design and synthesis of methyl-β-D-galactomalonyl phenyl esters as potent galectin-8*N* antagonists

Brijesh Patel, [†] *Chandan Kishor,* [†‡] *Todd. A. Houston,* [†] *Hadas Shatz-Azoulay,* [§] *Yehiel Zick,* [§] *Yaron Vinik,* [§*] *and Helen Blanchard* [†‡*]

[†]Institute for Glycomics, Griffith University, Gold Coast Campus, Queensland 4222, Australia.

[‡]School of Chemistry and Molecular Bioscience, and Molecular Horizons, University of Wollongong, Wollongong, New South Wales 2522, Australia.

[§]Department of Molecular Cell Biology, Weizmann Institute of Science, Rehovot 76100, Israel.

Corresponding authors

* E-mail: Helen_Blanchard@uow.edu.au

*E-mail: yaron.vinik@weizmann.ac.il

ABSTRACT

Galectin-8 is a β-galactoside recognizing protein having an important role in the regulation of bone remodeling, cancer progression and metastasis. Methyl-β-D-galactopyranoside malonyl aromatic esters have been designed to target and engage with particular amino acid residues of the galectin-8*N* extended carbohydrate-binding site. The chemically synthesized compounds had *in vitro* binding affinity towards galectin-8*N* in the range of 5-33 μM, as evaluated by isothermal titration calorimetry. This affinity directly correlated with the compounds' ability to inhibit galectin-8-induced expression of chemokines and proinflammatory cytokines in SUM159 breast cancer cell line. X-ray crystallographic structure determination revealed that these monosaccharide-based compounds bind galectin-8*N* by engaging its unique arginine (Arg59), and simultaneously cross-linking to another (Arg45) located across the carbohydrate-binding site. This structure-based drug design approach has led to discovery of novel monosaccharide galactose-based antagonists, with the strongest binding compound (K_d 5.72 μM) being 7-fold tighter than the disaccharide lactose.

INTRODUCTION

Galectin-8 is a member of the galectin family that comprises 15 mammalian lectins that bind β-galactosides through their carbohydrate recognition domains (CRD).[1] Based on their structural features, galectins are classified into three categories, termed proto type (galectin-1, -2, -5, -7, -10, -11, -13, -14, -15) that mainly exist as homodimers; tandem-repeat (galectin-4, -6, -8, -9, -12) that have two distinct CRDs joined by a variable length of polypeptide linker; and the chimera type galectin (galectin-3 (sole member)) which has only one CRD located at the C-terminus of the protein.[2-4] Galectin-8, like other galectins, is secreted by various cell types and act as matricellular proteins that ligate cell surface receptors and extracellular matrix (ECM) proteins to affect a wide range of biological functions including cell adhesion, migration, cell growth, apoptosis, and autophagy. Accordingly, galectin-8 expression is upregulated in cancerous tissue including lung, kidney, prostate, and breast.[5,6] Galectin-8-treated osteoblasts enhance expression of the osteoclastogenic factor receptor activator of nuclear factor kappa-B ligand (RANKL), which binds to the RANK receptor on osteoclasts and promotes osteoclastogenesis.[7,8] Galectin-8 plays important roles in rheumatic, autoimmune and inflammatory disorders, bone loss and osteoporosis.[7-10] It was recently reported that the galectin-8 treated primary cultures of murine osteoblasts trigger ~5-60 fold gene expression of several cytokines and chemokines including RANKL, monocyte chemoattractant protein-1 (MCP-1), stromal cell-derived factor 1 (SDF-1), interferon-γ-inducible protein 10 (IP-10), interleukin-6 (IL-6), interleukin-1β (IL-1β), and tumor necrosis factor-α (TNF-α).[11] Galectin-8 also increases ~4-fold protein levels of cytokines and chemokines, such as SDF-1 and MCP-1, in the culture medium of galectin-8 treated osteoblasts.[11] Galectin-8 increases SDF-1, MCP-1 gene expression in a number of cell types which promotes migration of cancer cells toward cells treated with this lectin.[11] Galectin-8, being an important

player in so many diseases, promoted us to design potent galectin-8 antagonists. Several galactose-based compounds, endogenous glycans have shown promising galectin-8*N* binding affinity such as fused tricyclic carbohydrate-benzene hybrid molecules (K_d 180 μM)[12], galactose-quinoline based compounds (K_d ~ 2 μM)[13], wild-type erythropoietin (EPO) glycoforms[14] produced in Chinese hamster ovary (CHO) cells (K_d 60 nM). Galectin-8's *N*-terminal ("galectin-8*N*″) and *C*-terminal ("galectin-8*C*″) CRDs share an overall amino acid sequence identity of 37%, but the amino acid residues Trp86, His65, Asn67, Arg69, Asn79, and Glu89 that are on the S4-S6 β-strands and form the carbohydrate-binding site region that recognizes the galactose portion of ligands, being identical in both CRDs. Important sequence differences do occur, most notably Arg45, Gln47, and Tyr141 in galectin-8*N* are replaced by Ser255, Asn257, and Asn348, respectively, in galectin-8*C*.[15] Between them, there are some important distinct characteristics, notably the presence of a unique arginine, Arg59, in galectin-8*N* which is absent in the galectin-8*C* binding site.[15] Galectin-8*N* and galectin-8*C* show different binding affinities for particular carbohydrate sequences.[16] For instance, galectin-8*N* demonstrated a 2.7 μM affinity for 3′-sialyllactose (3′-SiaLac) whereas galectin-8*C* has >1000 μM affinity.[17] An X-ray crystallographic study led to the explanation that the strong affinity with galectin-8*N* is due to the presence of its unique carbohydrate-binding site Arg59.[18] This finding prompted us to aim for a direct engagement with this amino acid as an approach to design potent galectin-8*N* antagonists that will serve as modulators or inhibitors of galectin-8 function. We have previously investigated methyl-3-*O*-[1-carboxyethyl]-β-D-galactopyranoside binding affinity and binding interactions with each CRD domain individually. This galactose-based compound showed 32 μM binding affinity with galectin-8*N* and no significant binding affinity with galectin-8*C*.[19] In this manuscript, we continue our drug design campaign and report the design and synthesis of galactose based methyl-β-D-

galactomalonyl phenyl esters, their binding affinity with galectin-8*N* CRD and their inhibition on galectin-8 mediated chemokines and proinflammatory cytokines expression in SUM159 breast cancer cells. Finally, protein X-ray crystallography was used to provide a structural basis for the mode of inhibition of galactomalonic acid derivatives at CRD of galectin-8*N*.

The galectin-8*N* CRD comprises two anti-parallel β-sheets forming a β-sandwich structure (Figure 1A).[18] The concave side of the CRD is formed by six β-strands (S1-S6) and contains amino acids that form the carbohydrate binding site, with the S4-S6 β-strands possessing amino acids that recognize the galactose portion of ligands. Galectin-8*N* preferentially recognizes oligosaccharides substituted with an anionic functional group such as 3′-sulfolactose and 3′-SiaLac.[17] This selective anionic recognition is due to the presence of the unique Arg59 on the S3-S4 loop (Figure 1A). The 3′-SiaLac carboxylic side chain forms a salt bridge interaction with Arg59, and a hydrogen bond with Gln47 (Figure 1B). Of further note, the S2 β-strand Tyr141 was identified as an important amino acid of the galectin-8*N* extended binding site because it forms van der Waals interaction with Lacto-*N*-fucopentaose-III (LNF-III) in the galectin-8*N*-LNF-III crystal structure.[18]

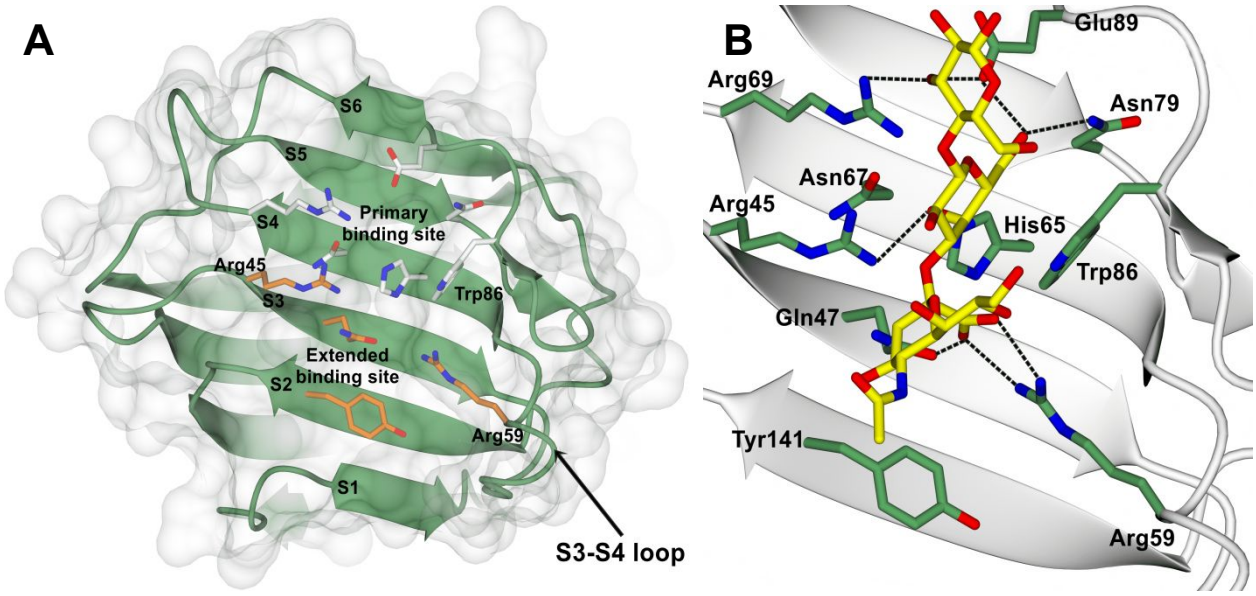

Figure 1. (A) Galectin-8*N* CRD. The illustration emphasizes the S1-S6 β-strands forming the concave face and the amino acids of the primary and extended carbohydrate binding sites. The Arg45 and Arg59 (in sticks; carbon atoms orange) are situated directly opposite to each other, highlighting their important positioning with respect to antagonist design. (B) The binding conformation of 3′-SiaLac (carbon atoms yellow) within the galectin-8*N* carbohydrate binding site (carbon atoms green) (PDB ID: 3AP7).[17]

The design of monosaccharide-based galectin-8*N* antagonists that we recently initiated, resulted in a galactose-based compound that interacts with Arg59 of galectin-8*N* with a binding affinity of 32 μM, equivalent to that of the disaccharide lactose.[19] Here we aim to design an antagonist which could cross-link both this arginine (Arg59), with that located across the binding site groove (Arg45), thus anchoring it from both sides. Further, we explore the enhancement of interactions with the extended binding site. To cross-link both arginines, we propose that two electron-rich functional groups to engage with the positively charged guanido groups of arginine would be needed. In light of this hypothesis we focused on the diketo functional group of malonic acid, which possess two electron rich carbonyl oxygens. Several synthetic and biological studies on diketo functional group-based compounds have been reported such as integrase[20,21], ribonuclease H[22] (RNase H), Hepatitis C Virus (HCV) RNA polymerase[23], malate synthetase[24], histone deacetylase (HDAC) inhibitor.[25,26] In these studies, it was observed that diketo oxygens of these compounds form a strong complex with the metal ion of the above enzymes and proved to be better inhibitors. Based on the knowledge of the three-dimensional structure of the carbohydrate binding

site of galectin-8*N* CRD, we have designed aromatic ring substituted galactomalonic acid in which it is supposed that the galactose portion would be recognized by the conserved amino acids of the binding site, the malonic oxygens are postulated to be able to cross-link the two arginines, and the aromatic ring is anticipated to make van der Waals interaction with tyrosine residue Tyr141. Malonic acid undergoes keto-enol tautomerism by the movement of its alpha hydrogens and the shifting of π-bonding electrons (Figure 2). Because of tautomerism, there is the possibility to generate stabilized enolate ions which have the ability to bind positively charged guanido group of arginines. This group offers a diverse "shape-shifting" array of hydrogen bond acceptors near the arginine residue.

Figure 2. Keto-enol tautomerism of galactomalonyl aromatic ester.

RESULTS AND DISCUSSION

In Silico Analysis of Interactions of Designed Compounds with Galectin-8*N*

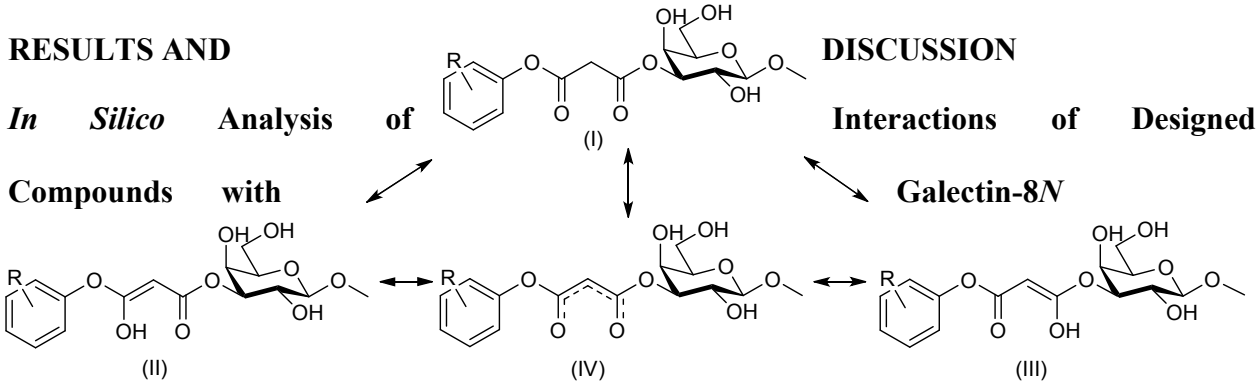

Following the rationale of incorporating a malonic acid group to develop potent galectin-8 antagonists, eight compounds of galactomalonic acid and derivatives were designed. A molecular

docking investigation was undertaken for these compounds with galectin-8*N* (PDB ID: 3AP7).[18] The key potential binding interactions that were consistent for these compounds with the galectin-8*N* carbohydrate binding site were revealed, as exemplified by the compound that was later evaluated to have the best binding affinity, the galactomalonyl aromatic ester **10** (Scheme 1, Page 10) (Figure 3).

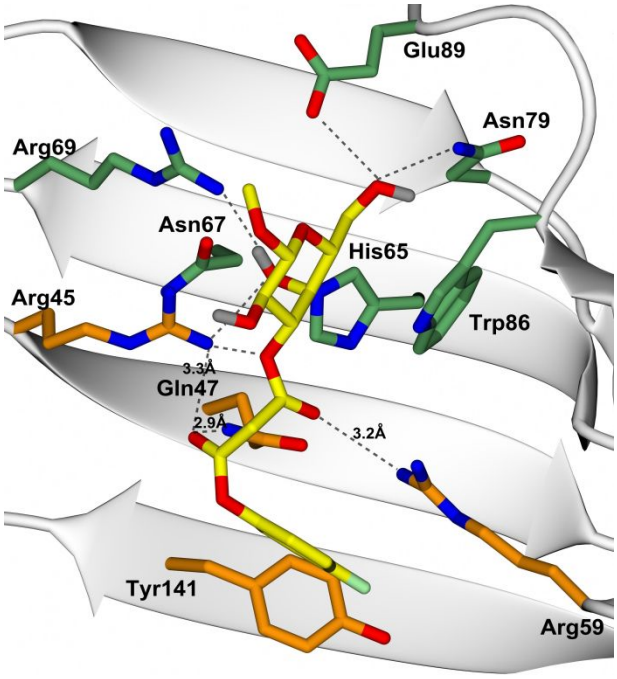

Figure 3. Docking conformation of galactomalonyl ester **10** within the galectin-8*N* binding site (PDB ID: 3AP7).[17]

The planar ring of the galactose portion was predicted to make van der Waals interactions with the aromatic tryptophan (Trp86) ring, whereas the free hydroxyls of the galactose interact with other conserved amino acids of the binding site. In this docked model, the malonic acid chain interacts with amino acids of the extended binding site in which there is feasibility for one carbonyl oxygen to make a potential salt-bridge (if ionized) or else a hydrogen-bonding interaction with

Arg59 (3.2 Å distance), and the second carbonyl oxygen potentially interacts with Arg45 and Gln47, with 3.3 Å and 2.9 Å distances respectively. In addition, the aromatic ring of the galactomalonyl ester **10** is predicted to make van der Waals interactions with Tyr141 as well as engage in a potential cation-π stacking with the Arg59 guanidinium group. The galectin-8*N*-galactomalonyl ester **10**, in its docked confirmation, shows potential for making the two important key interactions that we desired. One is the interaction of a negatively charged moiety with the unique Arg59, akin to that of carboxylic acid group of the 3′-siaLac in galectin-8*N*-3′-siaLac (PDB ID=3AP7);[18] and the second is the interaction with Tyr141 of the extended binding site, as exemplified by galactose of LNF-III in galectin-8*N*-LNF-III (PDB ID = 3AP9).[18]

Chemistry

The docking results supported that the designed compounds had potential to bind and engage with the unique Arg59. Steglich esterification was undertaken using either of two common coupling reagents *N,N*′-dicyclohexylcarbodiimide (DCC) and *N*-(3-dimethylaminopropyl)-*N*′-ethylcarbodiimide hydrochloride (EDCI), individually to synthesize the aromatic substituted galactose malonic esters **2-7** (Scheme 1) from methyl 4,6-di-*O*-benzylidene-2-*O*-methoxymethyl-β-D-galactopyranoside **1 (**synthesis described previously[19]).

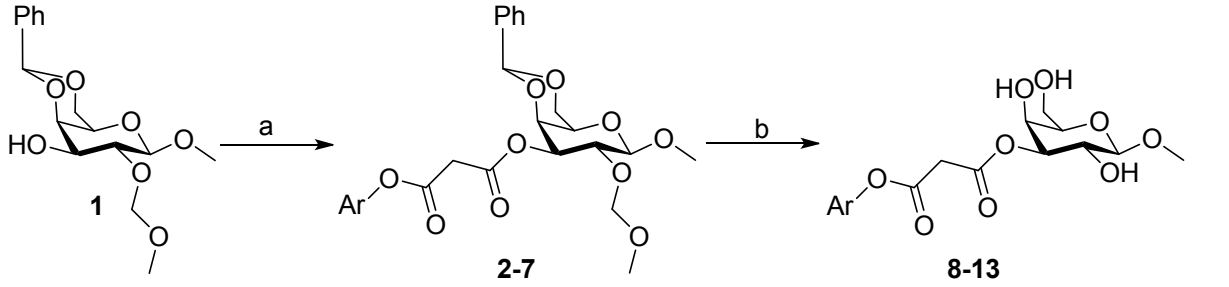

2 Ar=phenyl (87%)
3 Ar=4-methoxyphenyl (90%)
4 Ar=4-fluorophenyl (81%)
5 Ar=2,4-dichlorophenyl (90%)
6 Ar=3,5-dimethoxyphenyl (90%)
7 Ar=benzyl (90%)

8 Ar=phenyl (83%)
9 Ar=4-methoxyphenyl (86%)
10 Ar=4-fluorophenyl (85%)
11 Ar=2,4-dichlorophenyl (89%)
12 Ar=3,5-dimethoxyphenyl (90%)
13 Ar=benzyl (95%)

Scheme 1. Reagents and conditions: (a) DCC, aryl malonic acid **24-28, 30** (scheme S1), DMAP, DCM, -20 °C to room temperature, overnight (b) 60% aqueous acetic acid solution, 60 °C reflux for 4 h.

From reaction monitoring, it was observed that use of EDCI resulted in low conversion and low yield, whereas DCC acted as a better coupling reagent and completed the reaction in good yield. Different substituted phenyl malonic acids **24-28, 30** (synthesis, described in scheme S1) were prepared by reacting various substituted phenols with Meldrum's acid[27] and then these acids were used in a Steglich coupling reaction with the free 3-OH group of protected galactopyranoside.[28,29] Deprotection of ester intermediates was carried out by refluxing in 60% glacial acetic acid solution at 60 °C for 3 hours to give phenyl ring substituted galactomalonates **8-13.**[30] In the synthesis of galactomalonic acid **15**, the intermediate **7** was debenzylated by palladium catalyst with hydrogen gas to yield the malonic acid substituted galactopyranoside **14**.[31]

Deprotection of intermediate **14** in the presence of 60% acetic acid gave the malonic acid monoester of methyl β-galactopyranoside **15** (Scheme 2).

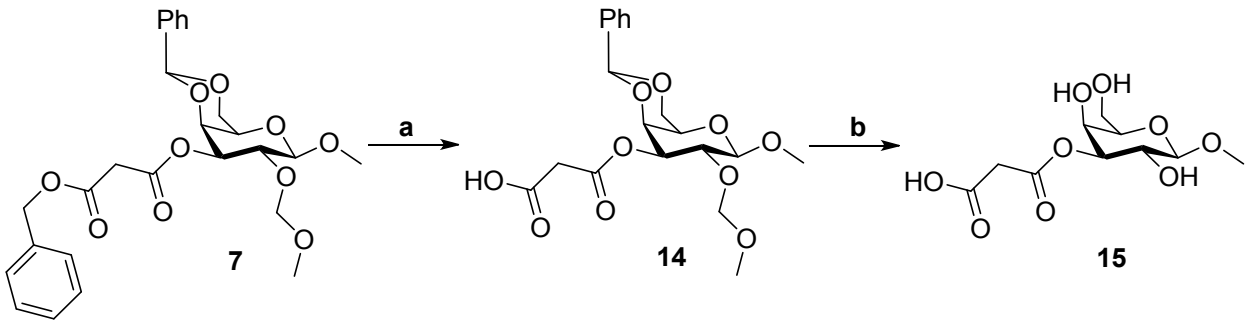

Scheme 2. Reagents and conditions: (a) 10% Pd/C, H_2 gas, anhydrous methanol (b) 60% aqueous acetic acid solution, 60 °C reflux for 4 h.

While this has the potential to decarboxylate at high temperature, malonate monoesters are stable to mildly acidic conditions at temperatures 60-70 °C.[32] The protected galactomalonyl methyl ester **16** was synthesized by nucleophilic substitution of methyl malonyl chloride with galactopyranoside **1** in the presence of organic base. Reaction was performed with three different bases: triethylamine (TEA), *N,N′*-diisopropylethylamine (DIPEA) and *N,N,N′,N′*-tetramethyl-1,2-ethylenediamine (TMEDA). Results showed that TEA, DIPEA gave lower conversion and lower yield compare to TMEDA. Deprotection of intermediate **16** was done by refluxing in 60% glacial acetic acid solution at 60 °C that gives methyl malonyl galactopyranoside ester **17** (Scheme 3).

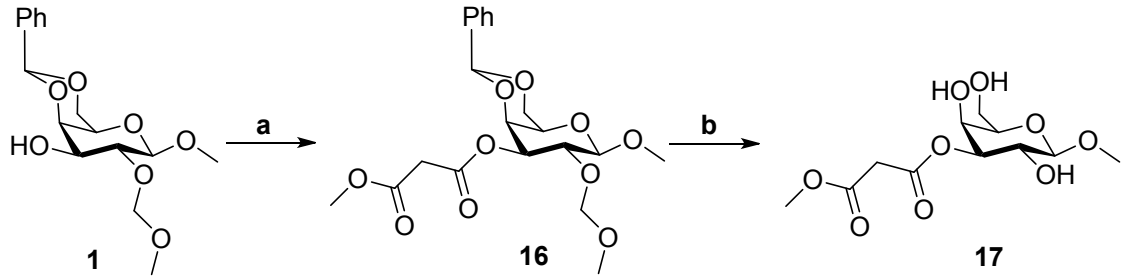

Scheme 3. Reagents and conditions: (a) TMEDA, methyl malonyl chloride, DCM, -20 °C to room temperature (b) 60% aqueous acetic acid solution, 60 °C reflux for 4 h.

Thermodynamic Analysis

Eight novel compounds were designed and synthesized, these are the galactomalonic acid **15** and its derivatives with aromatic substitution (compounds **8-13**), as well as an aliphatic methyl ester **17** (Figure 4).

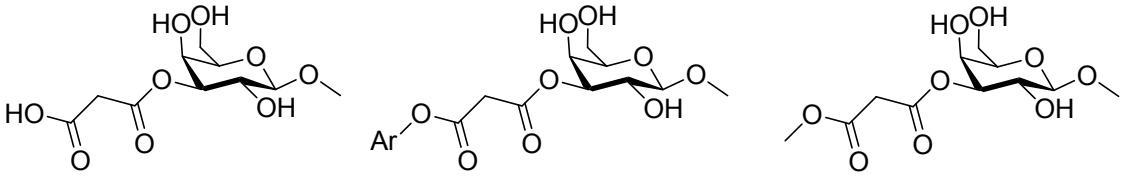

8 Ar=phenyl (83%)
9 Ar=4-methoxyphenyl (86%)
10 Ar=4-fluorophenyl (85%)
11 Ar=2,4-dichlorophenyl (89%)
12 Ar=3,5-dimethoxyphenyl (90%)
13 Ar=benzyl (95%)

Figure 4. Methyl-β-D-galactomalonic acid **15** and its derivative **8-13, 17.**

These compounds were evaluated for *in vitro* galectin-8*N* binding affinity by isothermal titration calorimetry (Table 1, Figure 5).

Table 1. Binding affinity and estimated thermodynamic parameters from ITC experiments

Compound	K_d (μM)	ΔH	-TΔS	ΔG	n
8	12.84 ±0.66	-14.63 ±0.4	-13.29	-27.92	0.81 ±0.02
9	9.47 ±0.43	-11.75 ±0.3	-16.93	-28.68	0.87 ±0.02
10	5.72 ±0.27	-13.63 ±0.2	-16.30	-29.93	0.89 ±0.02
11	11.89 ±0.56	-9.56 ±0.4	-18.54	-28.11	0.89 ±0.01
12	11.02 ±0.56	-11.98 ±0.2	-16.32	-28.30	0.81 ±0.05
13	9.17 ±0.67	-12.40 ±0.4	-17.26	-28.75	0.96 ±0.05
15	33.56 ±1.25	6.08 ±0.4	-31.6	-25.5	0.89 ±0.13
17	24.85 ±0.92	-7.068 ±0.6	-19.22	-26.28	0.80 ±0.15
Lac	37.92 ±1.27	-4.7 ±0.6	-20.5	-25.2	0.98 ±0.03
3'-SL	2.3 ±0.20	-51.8 ±0.8	19.64	-32.1	0.83 ±0.01

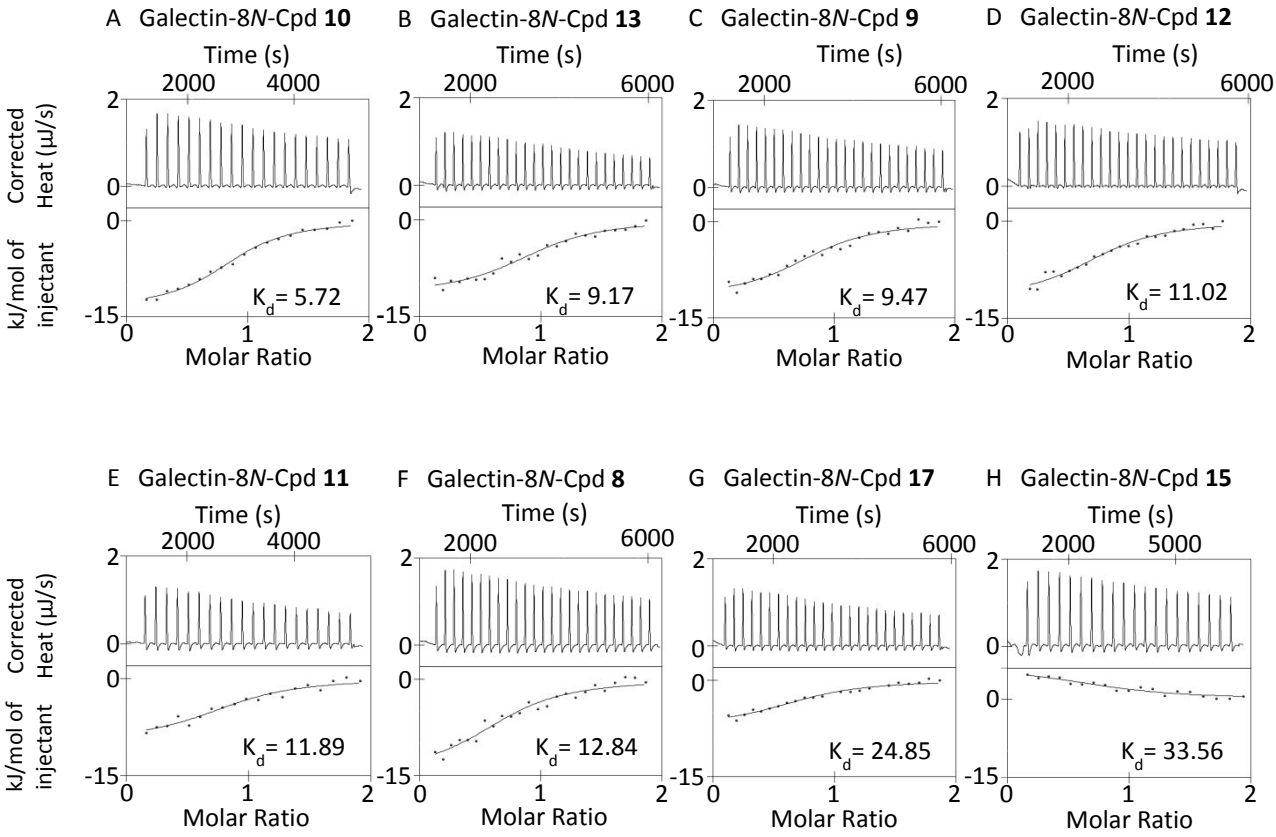

Figure 5. Isothermal titration calorimetric analysis. Binding isotherm for titration of 0.5 mM galactomalonyl ester **8-13, 17** (A-G) and 1mM galactomalonic acid **15** (H) with 100 μM galectin-8*N* in 20 mM Tris buffer at pH 7.5 containing 100 mM NaCl and 4 mM BME.

Galectin-8*N* shows 33.56 μM binding affinity for the monosaccharide galactomalonic acid **15**, which is slightly stronger than which we measured with the disaccharide lactose (37.92 μM). It shows a typical endothermic binding isotherm with unfavourable enthalpy difference in isothermal titration calorimetry (ITC) analysis (Figure 5H). When the electron-donating methyl group is introduced to the malonyl side chain this increased the affinity of the galactomalonic acid derivative **17** to 24.85 μM. From this, we can assume that the electron-donating group strengthens

the electron cloud associated with the carbonyl oxygens. Aromatic phenyl substitution of the galactomalonic acid derivative **8** shows almost three times better affinity (12.84 μM) than the parent galactomalonic acid **15,** and two times better than the methyl galactomalonyl ester **17**, giving strong evidence that the aromatic phenyl ring significantly enhances protein-ligand binding. This improvement may be due to interactions of the aromatic ring with the binding site for example by van der Waals interactions with Tyr141, cation-π stacking interaction with Arg59 and/or by making the oxygens of the malonyl group stronger nucleophiles. Introduction of fluoro substitution at the 4-position of the phenyl ring shows approximately 6-fold stronger binding affinity than galactomalonyl ester **15**. The 4-fluorophenyl substitution of galactomalonic acid (compound **10,** K_d 5.72 μM) presents the strongest binding monosaccharide galactose-based toward galectin-8*N* to date, with almost 7 times stronger binding affinity than lactose (37.92 μM) (Figure S1A). Addition of a methylene spacer group between the oxygen of malonyl and the aromatic phenyl ring produces the 9.17 μM affinity inhibitor **13**, which is slightly better than compound **8**. When an electron-donating 4-methoxy functional group is introduced to the *para* position on the phenyl ring, this increased binding affinity of galactomalonyl phenyl ester **9** to 9.47μM. Disubstitution on the phenyl ring shows 3-fold improved binding affinity over the galactomalonic acid **15**. For example, the 2,4-dichlorophenyl galactomalonyl ester **11**, containing electron-donating dichloro substitution, exhibits a 11.89 μM affinity and the 3,5-dimethoxyphenyl galactomalonyl ester **12**, containing dimethoxy substitution, shows 11.02 μM affinity, which suggests that disubstitution on the phenyl ring does not diminish the affinity of the overall compound and instead gives a slight enhancement over the phenyl substituted galactomalonic acid **8**. In addition to that, the different electronic effects of both dichloro and dimethoxy substituents to the phenyl ring do not create a significant difference in binding affinity of compound **11** and **12**. A molecular docking study of

disubstituted phenyl ring containing compounds shows that these substitutions do not create any steric hindrance in the binding site which could worsen the binding affinity of these compounds (Figure S2B and S2D). It also suggests that there is possibility of hydrogen bond interactions between the substituent of these compounds with Arg59 as represented (Figure S2D), which might be the reason for the slight improvement in binding affinity compared to the unsubstituted phenyl ring containing compound **8**.

Cytokine and Chemokine Expression Analysis

Galectin-8 upregulates cytokine and chemokine expression such as SDF-1, TNF-α, RANKL, IL-1β, MCP-1, IL-6 in osteoblasts extracted from calvariae of newborn CD1 mice.[11] A cell culture study was performed to determine the effects of the antagonists on galectin-8 induced expression of chemokines and inflammatory cytokines (IL-8, IL-1β, and IL-6) (Figure 6).

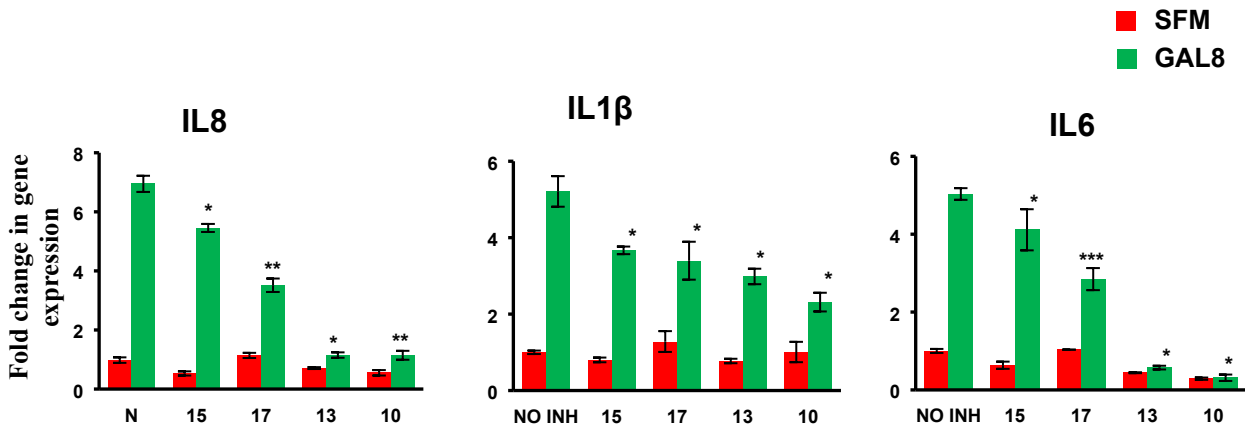

Figure 6. Effect of weak binding affinity compound **15, 17** and strong binding affinity compound **13, 10** on **IL8, IL1β and IL6** expression of SUM 159 breast cancer cell line in absence of galectin-

8 (SFM - red block) and presence of 50nM galectin-8 (green block). Results shown are means ± SEM of experiments done in duplicates (*p<0.05; **p<0.01; ***p<0.001).

SUM159 breast cancer cells were treated with or without 50 nM galectin-8, in the presence or absence of our weakest (**15**, **17**) or strongest (**13**, **10**) antagonists. As expected, treatment of SUM159 breast cancer cells with galectin-8 induced ~ 5-fold increased expresion of IL-8 (interleukin-8), IL-1β, and IL-6. Inclusion of the galectin-8 antagonists inhibited its effects, in correlation with the antagonists' affinity. Compounds with the strongest binding affinity (**10, 13**) showed more pronounced inhibition compared to the compounds having a weaker affinity (**15, 17**). Compound **10** showed 5-fold, 1.5-fold and 13-fold greater IL-8, IL-1β and IL-6 expression inhibition respectively than compound **15**. In comparison of weaker binding affinity compounds, compound **17** shows 1.5-fold IL-8, IL-6 expression inhibition than compound **15**. We further performed the dose-response relationship study of compound **10** and **13** at four different concentrations (1 μM, 10 μM, 100 μM and 500 μM) and observed that the lower concentration (1 μM) of both these compounds was able to inhibit galectin-8 induced IL-8 and IL-6 gene expression in SUM159 breast cancer cell line (Figure S3). It is clear from our analysis that in the absence of inhibitors the IL-6 and IL-8 expression is high, in the presence of weak inhibitors their expression is moderated, and in the presence of the best inhibitors (compounds **13** and **10**) expression is significantly lower.

Crystal Structure of Galectin-8*N* CRD in Complex with 13

Our X-ray crystallographic studies investigated binding interactions of **13** to galectin-8*N* (Figure 7). The galectin-8*N*-**13** complex structure was determined at 1.59 Å resolution (Table 2).

After initial refinement of galectin-8*N* CRD model, the difference electron density revealed unambiguous placement of the galactose ring portion of **13** facing the Trp86, and the galactose C3-hydroxy substituted benzyl malonic side chain within the galectin-8*N* extended binding site. The positive difference electron density that appears near the anomeric methoxy group and the C6 hydroxy group of galactose represents water molecules W1 and W2 respectively.

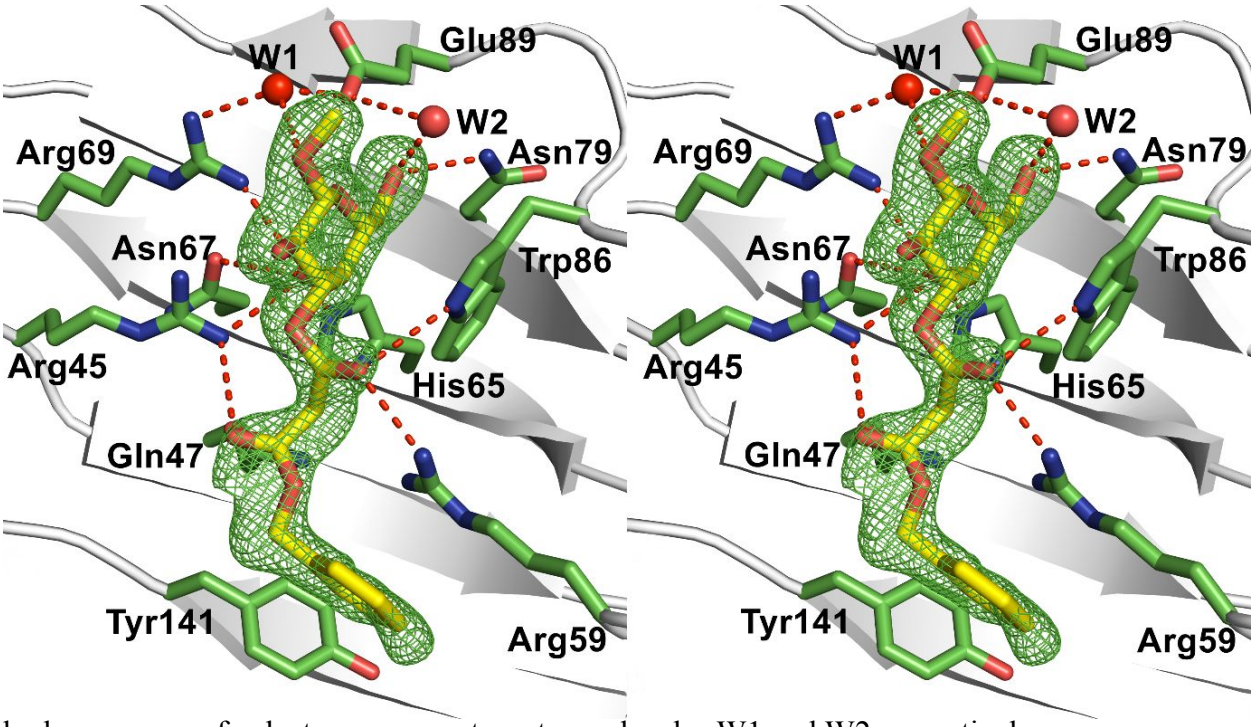

Figure 7. Stereo diagram of electron density map (green mesh) $2|F_o| - |F_c|$ α_c contoured at 1σ, for **13** (in sticks; carbon in yellow, oxygen in red) in complex with galectin-8*N* (gray cartoon) (PDB ID 6W4Z). Interacting side chain of amino acid residues of galectin-8*N* denoted as green sticks and the water molecules interacting with compound **13** indicated as red sphere.

Table 2. Crystallographic data and refinement statistics for the galectin-8*N*-13 structure

Data	Galectin-8*N*-13 complex
Indexing	
Crystal system, Space group	Monoclinic, C2
Unit cell	a= 110.39, b= 40.00, c= 70.32; α=89.96, β=98.22, γ=90.11
Merging and scaling	
Resolution [Å]	46.31-1.59
Total observations	280344 (13417) [a]
Unique observations	41190 (1987)
Multiplicity	6.8 (6.8)
Completeness [%]	99.9 (99.7)
I/σ	8.8 (2.5)
R_{merge} [%]	11.6 (153.8)
CC (1/2) [%]	0.997 (0.805)
Refinement	
R_{factor} [%]	19.25
R_{free} [%]	22.55
Number of atoms	
Protein	1211
Ligand	26
Water	58
Root mean square deviations	
Bond length [Å]	0.015
Bond angle [°]	1.90
Ramchandran plot statistics	
Favoured [%]	98.67
Allowed [%]	1.33
Average *B*-factor [Å^2]	
Protein	20.7
Ligand	43.6
Water	27.0
PDB ID	6W4Z
[a] Values in parenthesis are for the highest-resolution shell.	

Overall, the binding mode observed for the galactose portion of **13** is identical to the reported galectin-8*N*-lactose complex crystal structure in which the O4-hydroxy of galactose makes hydrogen bonds with His65, Asn67, Arg45, and Arg69, whereas the O6-hydroxy group engages in hydrogen bonding with Asn79 and Glu89. Two carbonyl groups of extended benzyl malonic acid cross link the two positively charged arginine Arg59 and Arg45, which is located across the binding site groove. This cross-linking interaction with arginine enables the inhibitor to be held from both sides. One carbonyl oxygen hydrogen-bonds with Trp86 and Arg59, whereas the second carbonyl oxygen hydrogen bonds with Arg45. This binding interaction validates the measured binding affinity of the parent compound **15** and its improved derivative structure **17** in which the electron-donating methyl group increased its binding affinity by increasing the nucleophilicity of the two carbonyl groups. The X-ray crystal structure of galectin-8*N*-**13** reveals two important interactions of the galectin-8*N* extended binding site amino acids which increase galactomalonyl phenyl esters binding affinity sharply from 33.56 μM to 12.84 μM. One is van der Waals interactions of Tyr141 with the phenyl ring, and the other is a cation-π stacking interaction of Arg59 with the phenyl ring. The galectin-8*N*-**13** X-ray crystal structure validates our design hypothesis and the predicted binding conformation from molecular docking, for compound **13.**

The X-ray crystallographic structure reveals the binding characteristics of galactomalonyl esters, which was able to explain molecular docking predicted binding energies of all other compounds. For example, galactomalonic acid **15** exhibits -5 kcal/mol and methyl ester **17** shows -5.4 kcal/mol, this small difference is probably due to the electron-donating effect of the methyl group which makes the two carbonyl oxygens of malonic acid stronger nucleophiles and observed to cross link with Arg45 and Arg59 in the crystal structure. When the aromatic phenyl ring was introduced to the malonyl substitution, these molecules show -6 to -7 kcal/mol binding energies

indicating stronger binding. From our X-ray crystallography study, it is very clear that the higher binding energies (tighter binding) of these compounds is due to the van der Waals interactions of the aromatic phenyl ring with Tyr141 as well as cation-π stacking with the Arg59.

CONCLUSIONS

We have designed a series of novel monosaccharide based galactomalonyl esters, subsequently chemically synthesized, and their binding affinities toward galectin-8*N* were analyzed. In addition, the binding mode and interactions of 18 with galectin-8*N* were elucidated based on their atomic structure, revealed by X-ray crystallography. This structure-based drug design approach has led to the discovery of novel monosaccharide galactose-based antagonists with single digit micromolar binding affinity (K_d 5.72-12.83 μM) with the strongest binding molecule (**10**) being 7-fold tighter than the disaccharide lactose. The malonyl substitution to the monosaccharide galactose generates compounds with a binding affinity almost equivalent to the disaccharide β-lactose, thus giving a novel scaffold for developing galectin-8 antagonists. Further, we discover that the aromatic phenyl ring substitution to the galactose malonic acid is the key factor in enhancing affinity. From the study of galectin-8's biological activities (assessed here by its stimulatory effects on cytokine/chemokine expression in cultured cell line) we concluded that the inhibitory effects of the antagonists directly correlate with their order of binding affinity to galectin-8*N*. Atomic structure, experimental binding affinities, and the cell culture results show that it is the aromatic malonyl substitution on the methyl β-D-galactopyranoside that leads to a sharp increase in binding affinity. The malonyl linker offers binding interactions that provide a novel approach to engineer potent galectin-8*N* antagonist.

EXPERIMENTAL SECTION

Chemistry: All reagents and solvents were dried prior to use according to standard methods. Commercial reagents were used without further purification. Analytical thin layer chromatography (TLC) was performed using on silica gel 60 F254 (Merck) with detection by UV absorption and/or by charring following immersion in a 5% ethanolic solution of sulfuric acid. Reaction products were purified using flash chromatography with silica gel 60 (0.040-0.063 mm). ^{1}H and ^{13}C NMR spectra were recorded at 298K using an Avance (400 MHz and 100 MHz respectively), spectrometer (Bruker Biospin) in solutions of deuterated chloroform ($CDCl_3$) or deuterated methanol (MeOH-D_4). Chemical shifts are reported to two decimal places in parts per millions (ppm) relative to tetramethylsilane (0 ppm). Electrospray ionization (ESI) low resolution mass spectrometry (LRMS) was performed using a Bruker Daltronics esquire 3000 Ion-Trap instruments, using Bruker Daltronics esquire control 5.0 software. All spectra were recorded in positive-ion mode at a concentration of 0.1-0.3 mg/mL. High Resolution Mass Spectra (HRMS) were measured by maXis II ETD to evaluate precise mass for novel synthesized derivatives. The purity of all final compounds was analysed by Thermo Fisher Scientific high performance liquid chromatography (HPLC), Accucore C18 column 2.1*150 mm, 2.6 micromolar. The detailed analytical condition is available in the supporting information. The purity of all analyzed compounds was found greater than 95%.

General Procedure for Preparation of Intermediates 2-7. A mixture of Methyl 4,6-di-*O*-benzylidene-2-*O*-methoxymethyl-β-D-galactopyranoside **1** (100 mg, 0.31 mmol, 1 equiv), aryl (Ar) malonic acid **24-28, 30** (0.46 mmol, 1.5 equiv), DCC (95 mg, 0.46 mmol, 1.5 equiv), and 4-dimethylaminopyridine (DMAP) (25 mg) in 15 mL dichloromethane (DCM) was stirred overnight

at -20 °C to room temperature. The reaction mixture was filtered and freeze to precipitate side product. Precipitated side product was filtered, and the filtrate was purified by column chromatography on silica gel (hexanes: ethyl acetate 3:1) to give intermediates **2-7**.

Methyl 4,6-di-*O*-benzylidene-2-*O*-methoxymethyl-3-*O*-[(3′-*O*-phenyl)malonyl]-β-D-galactopyranoside (2) Ar = phenyl, yield: 132 mg, 87%. ^{1}H NMR ($CDCl_3$, 400 MHz): δ 3.31 (s, 3H, H_3C-O-C1), 3.44 [s, 1H, $H_2C(CO)_2$], 3.50 (s, 3H, H_3C-O-CH_2), 3.60-3.62 [m, 2H, $H_2C(CO)_2$, H-6), 3.92-3.95 (m, 1H, H-5), 3.96-4.0 (m, 1H, H-2), 4.25 (d, *J* = 4.2 Hz, 1H, H-6), 4.30 (d, *J* = 8.3 Hz, 1H, H_2C-O-CH_3), 4.34 (d, *J* = 4.2 Hz, 1H, H-4), 4.62 (d, *J* = 8.2 Hz, 1H, H-1), 4.78 (d, *J* = 8.3 Hz, 1H, H_2C-O-CH_3), 4.94 (dd, *J* = 8.2 Hz, 4.3 Hz, 1H, H-3), 5.43 (s, 1H, HC-Ph), 6.95-6.97 (m, 2H, Ar), 7.13-7.15 (m, 1H, Ar), 7.19-7.21 (m, 2H, Ar), 7.23-7.25 (m, 3H, Ph), 7.39-7.42 (m, 2H, Ph). ^{13}C NMR ($CDCl_3$, 400 MHz): δ 41.5 [$CH_2(C{=}O)_2$], 55.9 (CH_3-O-C1), 56.9 (CH_3-O-CH_2), 66.0 (C-5), 68.9 (C-6), 72.7 (C-3), 73.4 (C-2), 74.6 (C-4), 97.2 (CH_2-O-CH_3), 101.1 (C-1), 103.9 (CH-Ph), 121.3 (2Ar), 126.2 (2Ar), 126.4 (2Ar), 128.1 (2Ar), 129.0 (2Ar), 129.5 (2Ar), 137.5 (Ar), 150.3 (Ar), 164.6 (C=O), 166.0 (C=O). ESIMS m/z [*M* + Na]$^{+}$ calcd for [$C_{25}H_{28}O_{10}Na$]$^{+}$: 511.2, found : 511.2.

Methyl 4,6-di-*O*-benzylidene-2-*O*-methoxymethyl-3-*O*-[(3′-*O*-{4-methoxyphenyl})malonyl]-β-D-galactopyranoside (3) Ar = 4-methoxyphenyl, yield: 145 mg, 90%. ^{1}H NMR ($CDCl_3$, 400 MHz): δ = 3.40 (s, 3H, H_3C-O-C1), 3.52 [d, *J* = 4.3 Hz, 1H, $H_2C(CO)_2$], 3.60 (s, 3H, H_3C-O-CH_2), 3.67 [d, *J* = 4.2 Hz, 2H, $H_2C(CO)_2$, H-6], 3.79 (s, 3H, H_3C-O-Ar), 4.01-4.05 (m, 1H, H-5), 4.08 (dd, *J* = 12.3 Hz, 4.1 Hz, 1H, H-2), 4.34 (d, *J* = 4.2 Hz, 1H, H-6), 4.39 (d, *J* = 12.3 Hz, 1H, H_2C-O-CH_3), 4.43 (d, *J* = 4.2 Hz, 1H, H-4), 4.71 (d, *J* = 4.3 Hz, 1H, H-1), 4.88 (d, *J* = 4.3 Hz, 1H, H_2C-O-CH_3), 5.05 (dd, *J* = 16.3 Hz, 4.2 Hz, 1H, H-3), 5.52 (s, 1H, HC-Ph), 6.76-6.79 (m, 2H, Ar), 6.94-6.96 (m, 2H, Ar), 7.33-7.35 (m, 3H, Ph), 7.49-7.52 (m, 2H, Ph). ^{13}C NMR (400 MHz,

$CDCl_3$): δ 41.5 [$CH_2(C{=}O)_2$], 55.5 (CH_3-O-C1), 55.9 (CH_3-O-CH_2), 56.9 (CH_3-O-Ar), 66.1 (C-5), 68.9 (C-6), 72.7 (C-3), 73.5 (C-2), 74.6 (C-4), 97.2 (CH_2-O-CH_3), 101.1 (C-1), 103.9 (CH-Ar), 114.4 (2Ar), 122.1 (2Ar), 126.4 (2Ar), 128.1 (2Ar), 129.0 (Ar), 137.5 (Ar), 143.8 (Ar), 157.4 (Ar), 165.0 (C=O), 166.0 (C=O). ESIMS m/z [*M* + Na]$^+$ calcd for [$C_{26}H_{30}O_{11}Na$]$^+$: 541.2, found : 541.3.

Methyl 4,6-di-*O*-benzylidene-2-*O*-methoxymethyl-3-*O*-[(3′-*O*-{4-fluorophenyl})malonyl]-β-D-galactopyranoside (4) Ar = 4-fluorophenyl, yield: 127 mg, 81%. ^{1}H NMR ($CDCl_3$, 400 MHz): δ 3.30 (s, 3H, H_3C-O-C1), 3.44-3.46 [m, 1H, $H_2C(CO)_2$], 3.51 (s, 3H, H_3C-O-CH_2), 3.58 [d, *J* = 4.2 Hz, 2H, $H_2C(CO)_2$, H-6], 3.91-3.95 (m, 1H, H-5), 3.99 (dd, *J* = 8.3 Hz, 4.2 Hz, 1H, H-2), 4.26 (s, 1H, H-6), 4.29 (d, *J* = 4.2 Hz, 1H, H_2C-O-CH_3), 4.34 (d, *J* = 4.1 Hz, 1H, H-4), 4.61 (d, *J* = 4.3 Hz, 1H, H-1), 4.78 (d, *J* = 8.2 Hz, 1H, H_2C-O-CH_3), 4.94 (dd, *J* = 16.2 Hz, 4.3 Hz, 1H, H-3), 5.42 (s, 1H, HC-Ph), 6.84-6.89 (m, 4H, Ar), 7.24-7.26 (m, 3H, Ph), 7.39-7.41 (m, 2H, Ph). ^{13}C NMR (400 MHz, $CDCl_3$): δ 41.5 [$CH_2(C{=}O)_2$], 55.9 (CH_3-O-C1), 57.0 (CH_3-O-CH_2), 66.0 (C-5), 68.9 (C-6), 72.7 (C-3), 73.4 (C-2), 74.7 (C-4), 97.3 (CH_2-O-CH_3), 101.2 (C-1), 103.9 (CH-Ph), 116.0 (2Ar), 122.7 (2Ar), 126.1 (2Ar), 128.1 (2Ar), 130.0 (Ar), 137.4 (Ar), 146.0 (Ar), 161.5 (Ar), 164.6 (C=O), 165.8 (C=O). ESIMS m/z [*M* + Na]$^+$ calcd for [$C_{25}H_{27}FO_{10}Na$]$^+$: 529.2, found : 529.2.

Methyl 4,6-di-*O*-benzylidene-2-*O*-methoxymethyl-3-*O*-[(3′-*O*-{2,4-dichlorophenyl})malonyl]-β-D-galactopyranoside (5) Ar = 2,4-dichlorophenyl, yield: 162 mg, 90%. ^{1}H NMR ($CDCl_3$, 400 MHz): δ 3.30 (s, 3H, H_3C-O-C1), 3.44-3.46 [m, 1H, $H_2C(CO)_2$], 3.51 (s, 3H, H_3C-O-CH_2), 3.64 [d, *J* = 4.3 Hz, 2H, $H_2C(CO)_2$, H-6], 3.93 (dd, *J* = 16.2 Hz, 4.3 Hz, 1H, H-2), 3.99 (dd, *J* = 16.2 Hz, 4.3 Hz, 1H, H-5), 4.26 (d, *J* = 12.3 Hz, 1H, H-6), 4.29 (d, *J* = 4.2 Hz, 1H, H_2C-O-CH_3), 4.35 (d, *J* = 4.3 Hz, 1H, H-4), 4.61 (d, *J* = 4.2 Hz,1H, H-1), 4.78 (d, *J* = 4.3 Hz, 1H, H_2C-O-CH_3), 4.92-4.96 (m, 1H, H-3), 5.42 (s, 1H, HC-Ph), 6.87-6.95 (m, 2H, Ar), 7.21-7.27 (m, 3H, Ph), 7.32

(s, 1H, Ar), 7.33-7.37 (m, 2H, Ph). ^{13}C NMR (400 MHz, $CDCl_3$): δ 41.1 [$CH_2(C{=}O)_2$], 55.9 (CH_3-O-C1), 57.0 (CH_3-O-CH_2), 66.0 (C-5), 68.9 (C-6), 72.7 (C-3), 73.4 (C-2), 74.7 (C-4), 97.2 (CH_2-O-CH_3), 101.0 (C-1), 103.9 (CH-Ar), 124.3 (Ar), 126.4 (Ar), 127.5 (Ar), 128.0 (3Ar), 128.1 (Ar), 129.1 (Ar), 130.0 (Ar), 132.3 (Ar), 137.5 (Ar), 145.2 (Ar), 163.5 (C=O), 165.4 (C=O). ESIMS m/z [*M* + Na]$^+$ calcd for [$C_{25}H_{26}Cl_2O_{10}Na$]$^+$: 579.2, found : 579.2.

Methyl 4,6-di-*O*-benzylidene-2-*O*-methoxymethyl-3-*O*-[(3′-*O*-{3,5-dimethoxyphenyl})malonyl]-β-D-galactopyranoside (6) Ar = 3,5-dimethoxyphenyl, yield: 160 mg, 90%. ^{1}H NMR ($CDCl_3$, 400 MHz): δ 3.30 (s, 3H, H_3C-O-C1), 3.44-3.46 [m, 1H, $H_2C(CO)_2$], 3.50 (s, 3H, H_3C-O-CH_2), 3.59 [d, *J* = 4.2 Hz, 2H, $H_2C(CO)_2$, H-6], 3.65 (s, 6H, 2H_3CO-Ar), 3.93 (dd, *J* = 16.3 Hz, 4.2 Hz, 1H, H-5), 3.99 (dd, *J* = 16.2 Hz, 4.3 Hz, 1H, H-2), 4.26 (d, *J* = 4.2 Hz, 1H, H-6), 4.29 (d, *J* = 8.3 Hz, 1H, H_2C-O-CH_3), 4.35 (d, *J* = 4.2 Hz, 1H, H-4), 4.62 (d, *J* = 8.3 Hz, 1H, H-1), 4.78 (d, *J* = 8.2 Hz, 1H, H_2C-O-CH_3), 4.93 (dd, *J* = 16.3 Hz, 4.2 Hz, 1H, H-3), 5.43 (s, 1H, HC-Ph), 6.18-6.19 (m, 2H, Ar), 6.25-6.26 (m, 1H, Ar), 7.22-7.24 (m, 3H, Ph), 7.38-7.41 (m, 2H, Ph). ^{13}C NMR (400 MHz, $CDCl_3$): δ 41.4 [$CH_2(C{=}O)_2$], 55.4 (2CH_3O-Ar), 55.9 (CH_3-O-C1), 57.0 (CH_3-O-CH_2), 66.0 (C-5), 68.9 (C-6), 72.6 (C-3), 73.4 (C-2), 74.7 (C-4), 97.2 (CH_2-O-CH_3), 98.7 (Ar), 99.9 (2Ar), 101.0 (C1), 103.9 (CH-Ar), 126.3 (2Ar), 128.0 (2Ar), 128.9 (Ar), 137.4 (Ar), 151.8 (Ar), 161.1 (2Ar), 164.4 (C=O), 166.0 (C=O). ESIMS m/z [*M* + Na]$^+$ calcd for [$C_{27}H_{32}O_{12}Na$]$^+$: 571.2, found : 571.2.

Methyl 4,6-di-*O*-benzylidene-2-*O*-methoxymethyl-3-*O*-[(3′-*O*-benzyl)malonyl]-β-D-galactopyranoside (7) Ar = benzyl, yield: 147 mg, 90%. ^{1}H NMR (MeOH-D_4, 400 MHz): δ 3.19 (s, 3H, H_3C-O-C1), 3.45 (s, 3H, H_3C-O-CH_2), 3.51 [s, 1H, $H_2C(CO)_2$], 3.71-3.76 [m, 1H, $H_2C(CO)_2$], 4.01 (d, *J* = 12.2 Hz, 1H, H-2), 4.10 (d, *J* = 12.2 Hz, 1H, H-5), 4.29 (d, *J* = 4.2 Hz, 1H, H_2C-O-CH_3), 4.32 (d, *J* = 12.3 Hz, 1H, H-4), 4.49 (d, *J* = 8.3 Hz, 1H, H-1), 4.66 (d, *J* = 8.3 Hz, 1H, H_2C-O-

CH_3), 4.91 (d, J = 4.3 Hz, 1H, H_2C-Ar), 4.93 (d, J = 8.2 Hz, 1H, H_2C-Ar), 4.99 (d, J = 12.3 Hz, 1H, H-3), 5.37 (s, 1H, HC-Ph), 7.21-7.25 (m, 5H, Ar), 7.26-7.28 (m, 3H, Ph), 7.35-7.37 (m, 2H, Ph). ^{13}C NMR (MeOH-D_4, 400 MHz): δ 33.3 (CH_2C=O), 54.9 (CH_3-OC1), 55.9 (CH_3-O-CH_2), 66.0 (C-5), 66.7 (CH_2O), 68.5 (C-6), 72.7 (C-3), 73.4 (C-2), 74.0 (C-4), 100.7 (CH_2-O-CH_3), 103.6 (C-1), 103.7 (CH-Ar), 126.0 (2Ar), 127.6 (2Ar), 127.7 (2Ar), 127.9 (2Ar), 128.1 (2Ar), 128.5 (Ar), 135.6 (Ar), 138.0 (Ar), 166.2 (C=O), 166.3 (C=O). ESIMS m/z [M + Na]$^+$ calcd for [$C_{26}H_{30}O_{10}Na$]$^+$: 525.2, found : 525.2.

Methyl 4,6-di-*O*-benzylidene-2-*O*-methoxymethyl-3-*O*-malonyl-β-D-galactopyranoside (14) Methyl 4,6-di-*O*-benzylidene-2-*O*-methoxymethyl-3-*O*-[(3′-*O*-benzyl)malonyl]-β-D-galactopyranoside **7** (180 mg, 0.36 mmol), was dissolved in anhydrous MeOH followed by addition of 10% Pd on activated carbon (60 mg) and stirred at room temperature in argon environment. After 5 min, hydrogen gas was passed continuously through balloon for 2 h. After 2 h, reaction mixture was filtered through celite as filtering agent and purified on silica column by using ethyl acetate: hexane (3:7) to yield product **14** (120 mg, 80%) as solids. ^{1}H NMR ($CDCl_3$, 400 MHz): δ 3.29 (s, 3H, H_3C-O-C1), 3.37 [d, J = 4.0 Hz, 2H, $H_2C(CO)_2$, H-6], 3.41 [s, 1H, $H_2C(CO)_2$], 3.48 (s, 3H, H_3C-O-CH_2), 3.88 (t, J = 8.3 Hz, 1H, H-2), 3.97 (dd, J = 12.3 Hz, 4.2 Hz, 1H, H-5), 4.24 (d, J = 4.3 Hz, 1H, H-6), 4.26 (d, J = 4.3 Hz, 1H, H_2C-O-CH_3), 4.28 (d, J = 4.3 Hz, 1H, H-4), 4.62 (d, J = 8.3 Hz, 1H, H-1), 4.75 (d, J = 4.2 Hz, 1H, H_2C-O-CH_3), 4.87 (dd, J = 12.2 Hz, 4.3 Hz, 1H, H-3), 5.40 (s, 1H, HC-Ph), 7.26-7.28 (m, 3H, Ar), 7.40-7.43 (m, 2H, Ar). ^{13}C NMR (400 MHz, $CDCl_3$): δ 40.9 [$CH_2(C=O)_2$], 55.8 (CH_3-O-C1), 56.9 (CH_3-O-CH_2), 66.0 (C-5), 68.8 (C-6), 72.8 (C-3), 73.7 (C-2), 74.5 (C-4), 100.9 (CH_2-O-CH_3), 103.8 (C-1), 103.8 (CH-Ar), 126.3 (2Ar), 128.1 (2Ar), 129.0 (Ar), 137.5 (Ar), 166.6 (C=O), 169.8 (C=O). ESIMS m/z [M + Na]$^+$ calcd for [$C_{19}H_{24}O_{10}Na$]$^+$: 435.2, found : 435.3.

Methyl 4,6-di-*O*-benzylidene-2-*O*-methoxymethyl-3-*O*-[(3′-*O*-methyl)malonyl]-β-D-galacto-pyranoside (16) Methyl 4,6-di-*O*-benzylidene-2-*O*-methoxymethyl-β-D-galactopyranoside **1** (100 mg, 0.306 mmol, 1 equiv), was dissolved in anhydrous DCM followed by addition TMEDA (229 µL, 1.53 mmol, 5 equiv) and stirred at -20 °C in argon environment. After 5 min, methyl malonyl chloride (98 µL, 0.918 mmol, 3 equiv) was added dropwise and stirred overnight room temperature. After 24 h, reaction mixture was filtered purified on silica column by using ethyl acetate: hexane (3:7) to yield product **16** (120 mg, 80%) as solids. ^{1}H NMR ($CDCl_3$, 400 MHz): δ 3.31 (s, 3H, H_3C-O-C1), 3.37 [d, J = 4.2 Hz, 2H, $H_2C(CO)_2$], 3.42 (d, J = 4.2 Hz, 1H, H-6), 3.49 (s, 3H, H_3C-O-CH_2), 3.58 (s, 3H, H_3C-OCO), 3.88 (t, J = 8.2 Hz, 1H, H-2), 3.99 (dd, J = 12.2 Hz, 4.3 Hz, 1H, H-5), 4.25 (d, J = 4.2 Hz, 1H, H-6), 4.28 (d, J = 4.2 Hz, 1H, H_2C-O-CH_3), 4.33 (d, J = 4.0 Hz, 1H, H-4), 4.61 (d, J = 8.2 Hz, 1H, H-1), 4.77 (d, J = 8.2 Hz 1H, H_2C-O-CH_3), 4.85 (dd, J = 8.2 Hz, 4.1 Hz, 1H, H-3), 5.43 (s, 1H, HC-Ph), 7.28-7.29 (m, 3H, HC-Ph), 7.42-7.45 (m, 2H, HC-Ph). ^{13}C NMR (400 MHz, $CDCl_3$): δ 41.2 [$CH_2(C{=}O)_2$], 52.5 (CH_3-COO), 55.8 (CH_3-O-C1), 56.9 (CH_3-O-CH_2), 66.0 (C-5), 68.9 (C-6), 72.6 (C-3), 73.3 (C-2), 74.5 (C-4), 97.2 (CH_2-O-CH_3), 101.0 (C-1), 103.9 (CH-Ar), 126.4 (2Ar), 128.1 (2Ar), 129.0 (Ar), 166.3 (C=O), 166.4 (C=O). ESIMS m/z [M + Na]$^+$ calcd for $[C_{20}H_{26}O_{10}Na]^+$: 449.2, found : 449.3.

General Procedure for Final Compounds 8-13, 15, and 17. Sugar **2-7, 14, 16** (100 mg) were dissolved in 60% aqueous acetic acid (6 mL) and refluxed at 60 °C. Reaction was quenched by addition of excess water, acetic acid was removed by toluene-chloroform mixture, concentrated and purified by column chromatography (DCM : MeOH, 97:3) to give **8-13, 15, 17**.

Methyl 3-*O*-[(3′-*O*-phenyl)malonyl]-β-D-galactopyranoside (8). Yield: 60 mg, 83%. ^{1}H NMR ($CDCl_3$, 400 MHz): δ 3.53 (s, 3H, H_3C-O-C1), 3.55-3.57 [m, 1H, $H_2C(CO)_2$], 3.66 (s, 1H,

H-4), 3.74 [s, 1H, $H_2C(CO)_2$], 3.78-3.81 (m, 1H, H-5), 3.82-3.84 (m, 1H, H-2), 3.87-3.91 (m, 2H, H-2, H-6), 4.22 (d, J = 4.2 Hz, 1H, H-6), 4.24 (d, J = 4.2 Hz, H-1), 4.84 (dd, J = 12.4 Hz, 4.2 Hz, 1H, H-3), 7.04-7.07 (m, 2H, Ar), 7.22 (s, 1H, Ar), 7.31-7.33 (m, 2H, Ar). ^{13}C NMR (400 MHz, $CDCl_3$): δ 41.5 [$CH_2(C=O)_2$], 57.3 (CH_3-O-C1), 62.8 (C-6), 67.8 (C-5), 68.9 (C-2), 73.7 (C-3), 104.1 (C-1), 121.2 (2Ar), 126.5 (Ar), 129.6 (2Ar), 150.0 (Ar), 165.5 (C=O), 166.4 (C=O). HRMS *m/z* [M + Na]$^+$ calcd for $[C_{16}H_{20}O_9Na]^+$: 379.1005, found: 379.0994.

Methyl 3-*O*-[(3′-*O*-{4-methoxyphenyl})malonyl]-β-D-galactopyranoside (9). Yield: 64 mg, 86%. ^{1}H NMR ($CDCl_3$, 400 MHz): δ 3.53 (s, 3H, H_3C-O-C1), 3.55-3.56 [m, 1H, $H_2C(CO)_2$], 3.64 (s, 1H, H-4), 3.71 [s, 1H, $H_2C(CO)_2$], 3.73 (s, 3H, H_3C-O-CH_2), 3.81 (dd, J = 12.2 Hz, 4.3 Hz, 1H, H-5), 3.88-3.89 (m, 1H, H-6), 3.90-3.92 (m, 1H, H-2), 4.17 (d, J = 4.3 Hz, 1H, H-6), 4.22 (d, J = 8.3 Hz, H-1), 4.82 (dd, J = 12.3 Hz, 4.2 Hz, 1H, H-3), 6.81-6.83 (m, 2H, 2H-Ar), 6.96-6.98 (m, 2H, 2H-Ar). ^{13}C NMR (400 MHz, $CDCl_3$): δ 41.4 [$CH_2(C=O)_2$], 55.6 (CH_3-O-Ar), 57.3 (CH_3-OC1), 62.7 (C-6), 67.7 (C-5), 68.9 (C-2), 73.7 (C-3), 104.1 (C-1), 114.6 (2Ar), 122.0 (2Ar), 143.6 (Ar), 157.7 (Ar), 165.6 (C=O), 166.8 (C=O). HRMS *m/z* [M + Na]$^+$ calcd for $[C_{17}H_{22}O_{10}Na]^+$: 409.1110, found: 409.1101.

Methyl 3-*O*-[(3′-*O*-{4-fluorophenyl})malonyl]-β-D-galactopyranoside (10). Yield: 63 mg, 85%. ^{1}H NMR ($CDCl_3$, 400 MHz): δ 3.54 (s, 3H, H_3C-O-C1), 3.62 [s, 1H, $H_2C(CO)_2$], 3.68 (s, 1H, H-4), 3.72 [s, 1H, $H_2C(CO)_2$], 3.84-3.85 (m, 1H, H-5), 3.86-3.88 (m, 1H, H-6), 3.89-3.91 (m, 1H, H-2), 4.18 (d, J = 4.3 Hz, 1H, H-6), 4.22 (d, J = 8.2 Hz, H-1), 4.84 (dd, J = 12.3 Hz, 4.2 Hz, 1H, H-3), 6.81-6.83 (m, 2H, Ar), 6.96-6.98 (m, 2H, Ar). ^{13}C NMR (400 MHz, $CDCl_3$): δ 41.4 [$CH_2(C=O)_2$], 57.4 (CH_3-O-C1), 62.8 (C-6), 67.9 (C-5), 68.9 (C-2), 73.7 (C-3), 104.1 (C-1), 116.2 (2Ar), 122.7 (Ar), 122.8 (2Ar), 160.0 (Ar), 165.4 (C=O), 166.2 (C=O). HRMS *m/z* [M + Na]$^+$ calcd for $[C_{16}H_{19}FO_9Na]^+$: 397.0910, found: 397.0901.

Methyl 3-*O*-[(3′-*O*-{2,4-dichlorophenyl})malonyl]-β-D-galactopyranoside (11). Yield: 68 mg, 89%. ^{1}H NMR (MeOH-D_4, 400 MHz): δ 3.26 (s, 3H, H_3C-O-C1), 3.43-3.44 [m, 3H, $H_2C(CO)_2$, H-4], 3.48 (dd, *J* = 4.2 Hz, 2.3 Hz, 1H, H-5), 3.62-3.65 (m, 1H, H-6), 3.70-3.75 (m, 1H, H-4), 3.98 (dd, *J* = 16.2 Hz, 2.3 Hz, 1H, H-2), 4.24 (t, *J* = 8.3 Hz, 1H, H-6), 4.55 (dd, *J* = 12.2 Hz, 4.3 Hz, H-1), 4.71 (dd, *J* = 8.3 Hz, 4.2 Hz, 1H, HO-C6), 4.80 (dd, *J* = 8.3 Hz, 4.2 Hz, 1H, H-3), 6.76-6.78 (m, 1H, H-Ar), 7.0-7.02 (m, 1H, H-Ar), 7.18-7.21 (m, 1H, H-Ar), 7.28-7.31 (m, 1H, H-Ar), 7.48-7.49 (m, 1H, H-Ar). ^{13}C NMR (MeOH-D_4, 400 MHz): δ 54.7 [$CH_2(C{=}O)_2$], 55.8 (CH_3-O-C1), 60.6 (C-6), 66.2 (C-4), 73.2 (C-2), 74.6 (C-3), 76.3 (C-5), 96.6 (C-1), 104.1 (Ar), 117.1 (Ar), 121.1 (Ar), 127.4 (Ar), 128.9 (Ar), 152.1 (Ar), 166.4 (C=O), 167.3 (C=O). HRMS *m/z* [*M* + Na]$^+$ calcd for $[C_{16}H_{18}Cl_2O_9Na]^+$: 447.0225, found: 447.0247.

Methyl 3-*O*-[(3′-*O*-{3,5-dimethoxyphenyl})malonyl]-β-D-galactopyranoside (12). Yield: 68 mg, 90%. ^{1}H NMR ($CDCl_3$, 400 MHz): δ 3.53 (s, 3H, H_3C-O-C1), 3.54-3.56 [m, 1H, $H_2C(CO)_2$], 3.64 (s, 1H, H-4), 3.71 (s, 6H, $2H_3CO$-Ar), 3.72 [s, 1H, $H_2C(CO)_2$], 3.81 (dd, *J* = 12.3 Hz, 4.2 Hz, 1H, H-5), 3.86-3.87 (m, 1H, H-6), 3.88-3.91 (m, 1H, H-2), 4.17 (d, *J* = 4.3 Hz, 1H, H-6), 4.23 (d, *J* = 8.2 Hz, 1H, H-1), 4.83 (dd, *J* = 8.2 Hz, 4.3 Hz, 1H, H-3), 6.22-6.23 (m, 2H, 2H-Ar), 6.28-6.30 (m, 1H, H-Ar). ^{13}C NMR (400 MHz, $CDCl_3$): δ 41.5 [$CH_2(C{=}O)_2$], 55.5 ($2CH_3$-O-Ar), 57.3 (CH_3-O-C1), 62.7 (C-6), 67.8 (C-5), 68.9 (C-2), 73.7 (C-3), 98.7 (C-1), 99.9 (2Ar), 104.1 (Ar), 151.6 (Ar), 161.2 (2Ar), 165.5 (C=O), 166.1 (C=O). HRMS *m/z* [*M* + Na]$^+$ calcd for $[C_{18}H_{24}O_{11}Na]^+$: 439.1216, found: 439.1201.

Methyl 3-*O*-[(3′-*O*-benzyl)malonyl]-β-D-galactopyranoside (13). Yield: 70 mg, 95%. ^{1}H NMR ($CDCl_3$, 400 MHz): δ 3.56 (s, 3H, H_3C-O-C1), 3.57-3.59 [m, 1H, $H_2C(CO)_2$], 3.72-3.77 (m, 3H, H-2, H-5, H-6), 4.06 (d, *J* = 4.3 Hz, 1H, H-6), 4.26 (d, *J* = 8.3 Hz, 1H, H-1), 4.79 (dd, *J* = 12.2 Hz, 4.2 Hz, 1H, H-3), 5.20 (s, 2H, H_2C-Ar), 7.33-7.42 (m, 5H, 5H-Ar). ^{13}C NMR (400 MHz,

$CDCl_3$): δ 47.6 (CH_2C=O), 54.9 (CH_3-O-C1), 60.7 (C-5), 66.2 (CH_2O), 66.7 (C-6), 68.4 (C-3), 74.8 (C-2), 77.1 (C-4), 104.4 (C-1), 127.8 (2Ar), 127.9 (2Ar), 128.1 (Ar), 135.6 (Ar), 166.6 (C=O), 166.9 (C=O). HRMS *m/z* [*M* + Na]$^+$ calcd for $[C_{16}H_{20}O_9Na]^+$: 393.1161, found: 393.1150.

Methyl 3-*O*-malonyl-β-D-galactopyranoside (15). Yield: 61 mg, 90%. ^{1}H NMR (MeOH-D_4, 400 MHz): δ 3.38-3.40 [m, 1H, $H_2C(C=O)_2$], 3.44 (s, 3H, H_3C-O-C1), 3.49-3.52 [m, 1H, $H_2C(C=O)_2$], 3.63-3.66 (m, 1H, H-4), 3.66-3.68 (m, 1H, H-5), 4.02 (d, *J* = 4.2 Hz, 1H, H-6), 4.17 (d, *J* = 8.2 Hz, 1H, H-6), 4.62 (dd, *J* = 12.2 Hz, 4.2 Hz, 1H, H-3). HRMS *m/z* [*M* + Na]$^+$ calcd for $[C_{10}H_{16}O_9Na]^+$: 303.0692, found: 303.0707.

Methyl 3-*O*-[(3′-*O*-methyl)malonyl]-β-D-galactopyranoside (17). Yield: 60 mg, 87%. ^{1}H NMR ($CDCl_3$, 400 MHz): δ 3.42 [s, 2H, $H_2C(C=O)_2$], 3.53 (s, 3H, H_3C-O-C1), 3.54-3.57 (m, 2H, H-4, H-5), 3.71 (s, 3H, H_3C-OCO), 3.81-3.84 (m, 1H, H-6), 3.87 (dd, *J* = 12.3 Hz, 4.2 Hz, 1H, H-2), 3.93 (dd, *J* = 12.3 Hz, 4.2 Hz, 1H, HO-C6), 4.17 (d, *J* = 4.0 Hz, 1H, H-6), 4.22 (d, *J* = 4.0 Hz, 1H, H-1), 4.78 (dd, *J* = 12.3 Hz, 4.2 Hz, 1H). ^{13}C NMR (400 MHz, MeOH-D_4): δ 47.0 [$CH_2(C=O)_2$], 51.5 (H_3CO-CO), 55.9 (CH_3-OC1), 60.6 (C-6), 66.2 (C-4), 68.3 (C-2), 74.8 (C-3), 77.0 (C-5), 104.4 (C-1), 166.6 (C=O), 167.6 (C=O). HRMS *m/z* [*M* + Na]$^+$ calcd for $[C_{11}H_{18}O_9Na]^+$: 317.0848, found: 317.0837.

Molecular Docking

The published crystal structure (PDB ID = 3AP7)[18] of the galectin-8*N* CRD with bound 3′-SiaLac was used for the modelling study of our designed aryl substituted galactomalonic acid compounds. Protein coordinate files were prepared by removing water molecules, the addition of polar hydrogen and Kollman charges via AutoDock Tools (ADT).[33] Designed compounds were drawn in Marvin sketch, followed by energy minimization by PRODRG web server.[34] The grid

map was created with 54, 60 and 48 points in each x, y and z direction respectively with 1 Å spacing. Molecular docking was performed by use of AutoDock Vina software[35] and the docked confirmations were individually analyzed to determine the possible binding poses. Validation of molecular docking method was carried out by performing redocking of 3′-SiaLac in the binding site. Figures were generated using CCP4mg.[36]

Isothermal Titration Calorimetry (ITC)

Quantitation of the binding affinity was done by measuring the dissociation constant using Nano ITC Instrument (Micro Cal, TA). The galectin-8*N* (residues 8-154) protein was expressed in an untagged form as described previously.[37] Briefly, the bacterial culture was induced with Isopropyl β-D-1-thiogalactopyranoside (IPTG) for 4 h at room temperature and purified using affinity chromatography on a lactosyl-Sepharose column at 4 °C. For the ITC study, galectin-8*N* protein and ligand solutions were prepared by mixing stock solution with Tris buffer (20 mM Tris pH 7.5, 100 mM NaCl, 4 mM BME, 5% DMSO). Samples were degassed prior to use. Titrations were performed in TA Nano Analyze calorimeter using 20-25 injections applied at an interval of 150 seconds at 298 K. Each injection dispensed 2.5 µl of ligand into the sample cell containing 300 µl of Galectin-8*N* at 200 rpm. Ligand titration and blank data were collected at room temperature, and binding isotherms were fitted using an independent model in the NanoAnalyzeTM v3.7 software.

Cell culture study

Human breast cancer cell (SUM159, triple negative) line was purchased from the American Type Culture Collection (ATCC). SUM159 cell line was cultured in RPMI medium supplemented

with 10% fetal bovine serum (FBS) and 100 U/mL penicillin/streptomycin B, in a humidified 37 °C incubator with 5% CO_2. SUM 159 cells were seeded at 50000 cells/cm^2 in 12-well tissue culture plates. Cells were incubated with the indicated compounds (500 μM) with or without 50 nM of galectin-8 for 24 h. Next, the cells were harvested, and total RNA was extracted using the PerfectPure RNA kit (5 PRIME). RNA was quantified, and cDNA was generated by cDNA Reverse Transcription kit (Applied Biosystems) following manufacturer instructions. Quantitative detection of mRNA transcripts was carried out by real-time PCR using ABI-Prism 7300 instrument (Applied Biosystems) using SYBR Green PCR mix (Invitrogen) and specific primers (400 nM final concentration).[11] Results were normalized to mRNA levels of glyceraldehyde-3-phosphate dehydrogenase (GAPDH; human).

Crystallization and Structure Determination

The galectin-8*N*-**13** complex structure was obtained by soaking the apo galectin-8*N* crystals for 3 h in 10 mM of **13**. The apo galectin-8*N* crystals were generated in 1X Tris buffer saline (50 mM Tris, 150 mM sodium chloride, Tris-HCl) and Hampton crystal screen condition 40 (0.1M sodium citrate dihydrate pH 5.6, 20% PEG 4000, 10% IPA). Compound **13** was dissolved in the condition 40 solution at a concentration of 10 mM and soaked into the apo crystals for 3 h. X-ray diffraction data were remotely collected at the Australian Synchrotron using Blu-Ice software[38] at 100 K with a wavelength of 0.9537 Å, and Eiger detector. The data were integrated using the XDS software package,[39] and the space group determination and scaling of the data was performed using AIMLESS.[40] Molrep[41] implemented in CCP4[42] was used for molecular replacement with the apo galectin-8*N* (PDB ID: 5T7S)[37] structure used as the search model. The chemical information file

for **13** was generated using the PRODRG server.[34] Refinement was carried out using REFMAC5,[43] model building, and visualization done in COOT.[44]

ASSOCIATED CONTENT

Supporting Information

Additional figures illustrating ITC graph of reference compounds, molecular docking analysis of key compounds, chemical intermediate synthetic scheme and procedure, ^{1}H and ^{13}C NMR spectra, HRMS spectra and chromatography analysis of key compounds

Accession Codes

PDB code for galectin-8*N*- Methyl 3-*O*-[(3′-*O*-benzyl)malonyl]-β-D-galactopyranoside **13** complex is 6W4Z. Authors will release the atomic coordinates and experimental data upon article publication.

Molecular Docking coordinates

Galectin-8*N*-compound **10**, **11**, **12**, **13**, **17** complexes. Authors will release the atomic coordinates upon article publication.

AUTHOR INFORMATION

Corresponding Authors

*E-mail: Helen_Blanchard@uow.edu.au

*E-mail: yaron.vinik@weizmann.ac.il

ORCID

Helen Blanchard: 0000-0003-3372-5027

Brijesh Patel: 0000-0002-8029-0356

Chandan Kishor: 0000-0002-6328-1116

Author Contributions

H.B. directed the research study. B.P. performed all experiments including protein expression, purification, ITC study, crystallization and structure determination with advice from C.K and H.B., chemical synthesis and characterization of compounds with advice from T.H. B.P. performed cell culture study at Weizmann Institute of science with advice from H.S, Y.V and Y.Z. Initial draft of the manuscript was undertaken by B.P with revisions by H.B, and all authors subsequently reviewed and contributed to the manuscript.

ACKNOWLEDGEMENTS

H.B gratefully acknowledges financial support from the Cancer Council Queensland (ID 1080845). B.P is supported by Griffith University GUPRS and GUIPRS scholarship. The MX2 beamline scientists at the Australian Synchrotron, Melbourne, Australia are acknowledged for their support during X-ray diffraction data collection.

ABBREVIATIONS USED

RANKL, receptor activator of nuclear factor kappa-B ligand; ECM, extracellular matrix; SDF-1, stromal cell-derived factor-1; MCP-1, monocyte chemoattractant protein-1; IP-10, interferon-γ-inducible protein-10; IL-6, interleukin-6; IL-1β, interleukin-1β; TNF-α, tumor necrosis factor-α;

IL-8, interleukin-8; LNF-III, lacto-N-fucopentaose-III; 3′-SiaLac, 3′-sialyllactose; HDAC, histone deacetylase; HCV, Hepatitis C Virus; ITC, isothermal titration calorimetry; DCM, dichloromethane; TMEDA, tetramethyl ethylenediamine; DIPEA, diisopropylethylamine; DMAP, 4-dimethylaminopyridine; TEA, triethylamine; DCC, N,N′-dicyclohexylcarbodiimide; EDCI, *N*-(3-dimethylamino-propyl)-*N*′-ethylcarbodiimide hydrochloride; TLC, thin layer chromatography; ADT, AutoDock Tools; IPTG, Isopropyl-β-D-1-thiogalactopyranoside; BME, β-mercaptoethanol. HPLC, high performance liquid chromatography; ATCC, American Type Culture Collection; FBS, fetal bovine serum; GAPDH, glyceraldehyde-3-phosphate dehydrogenase.

REFERENCES:

1. Di Lella, S.; Sundblad, V.; Cerliani, J. P.; Guardia, C. M.; Estrin, D. A.; Vasta, G. R.; Rabinovich, G. A. When galectins recognize glycans: from biochemistry to physiology and back again. *Biochemistry* **2011**, *50* (37), 7842-7857.
2. Rabinovich, G. A.; Vidal, M. Galectins and microenvironmental niches during hematopoiesis. *Current Opinion in Hematology* **2011**, *18* (6), 443-451.
3. Thiemann, S.; Baum, L. G. The road less traveled: regulation of leukocyte migration across vascular and lymphatic endothelium by galectins. *Journal of Clinical Immunology* **2011**, *31* (1), 2-9.
4. Ledeen, R. W.; Wu, G.; André, S.; Bleich, D.; Huet, G.; Kaltner, H.; Kopitz, J.; Gabius, H. J. Beyond glycoproteins as galectin counterreceptors: tumor-effector T cell growth control via ganglioside GM1. *Annals of the New York Academy of Sciences* **2012**, *1253* (1), 206-221.

5. Elola, M. T.; Ferragut, F.; Cardenas Delgado, V. M.; Nugnes, L. G.; Gentilini, L.; Laderach, D.; Troncoso, M. F.; Compagno, D.; Wolfenstein-Todel, C.; Rabinovich, G. A. Expression, localization and function of galectin-8, a tandem-repeat lectin, in human tumors. *Histology and histopathology* **2014**, *29* (9), 1093-1105.
6. Compagno, D.; Gentilini, L. D.; Jaworski, F. M.; Pérez, I. G.; Contrufo, G.; Laderach, D. J. Glycans and galectins in prostate cancer biology, angiogenesis and metastasis. *Glycobiology* **2014**, *24* (10), 899-906.
7. Vinik, Y.; Shatz-Azoulay, H.; Vivanti, A.; Hever, N.; Levy, Y.; Karmona, R.; Brumfeld, V.; Baraghithy, S.; Attar-Lamdar, M.; Boura-Halfon, S.; Bab, I.; Zick, Y. The mammalian lectin galectin-8 induces RANKL expression, osteoclastogenesis, and bone mass reduction in mice. *eLife* **2015**, *4*, e05914.
8. Vinik, Y.; Shatz-Azoulay, H.; Hiram-Bab, S.; Kandel, L.; Gabet, Y.; Rivkin, G.; Zick, Y. Ablation of the mammalian lectin galectin-8 induces bone defects in mice. *The FASEB Journal* **2018**, *32* (5), 2366-2380.
9. Nishi, N.; Shoji, H.; Seki, M.; Itoh, A.; Miyanaka, H.; Yuube, K.; Hirashima, M.; Nakamura, T. Galectin-8 modulates neutrophil function via interaction with integrin alphaM. *Glycobiology* **2003**, *13* (11), 755-763.
10. Eshkar Sebban, L.; Ronen, D.; Levartovsky, D.; Elkayam, O.; Caspi, D.; Aamar, S.; Amital, H.; Rubinow, A.; Golan, I.; Naor, D.; Zick, Y.; Golan, I. The involvement of CD44 and its novel ligand galectin-8 in apoptotic regulation of autoimmune inflammation. *Journal of immunology (Baltimore, Md. : 1950)* **2007**, *179* (2), 1225-1235.

11. Shatz-Azoulay, H.; Vinik, Y.; Isaac, R.; Koehler, U.; Lev, S.; Zick, Y. The animal lectin galectin-8 promotes cytokine expression and metastatic tumor growth in mice. *Scientific Reports* **2020,** *10*(1), 7375

12. Wu, C.; Yong, C.; Zhong, Q.; Wang, Z.; Nilsson, U. J.; Zhang, Y. Synthesis of tricyclic carbohydrate–benzene hybrids as selective inhibitors of galectin-1 and galectin-8*N*-terminal domains. *RSC Advances* **2020**, *10* (33), 19636-19642.

13. Pal, K. B.; Mahanti, M.; Huang, X.; Persson, S.; Sundin, A. P.; Zetterberg, F. R.; Oredsson, S.; Leffler, H.; Nilsson, U. J. Quinoline–galactose hybrids bind selectively with high affinity to a galectin-8 N-terminal domain. *Organic & Biomolecular Chemistry* **2018**, *16* (34), 6295-6305.

14. Nielsen, M. I.; Stegmayr, J.; Grant, O. C.; Yang, Z.; Nilsson, U. J.; Boos, I.; Carlsson, M. C.; Woods, R. J.; Unverzagt, C.; Leffler, H.; Wandall, H. H. Galectin binding to cells and glycoproteins with genetically modified glycosylation reveals galectin-glycan specificities in a natural context. *Journal of Biological Chemistry* **2018**, *293* (52), 20249-20262.

15. Kumar, S.; Frank, M.; Schwartz-Albiez, R. Understanding the specificity of human galectin-8*c* domain interactions with its glycan ligands based on molecular dynamics simulations. *PLOS ONE* **2013**, *8* (3), e59761.

16. Carlsson, S.; Öberg, C. T.; Carlsson, M. C.; Sundin, A.; Nilsson, U. J.; Smith, D.; Cummings, R. D.; Almkvist, J.; Karlsson, A.; Leffler, H. Affinity of galectin-8 and its carbohydrate recognition domains for ligands in solution and at the cell surface. *Glycobiology* **2007**, *17* (6), 663-676.

17. Ideo, H.; Seko, A.; Ishizuka, I.; Yamashita, K. The *N*-terminal carbohydrate recognition domain of galectin-8 recognizes specific glycosphingolipids with high affinity. *Glycobiology* **2003**, *13* (10), 713-723.

18. Ideo, H.; Matsuzaka, T.; Nonaka, T.; Seko, A.; Yamashita, K. Galectin-8-*N*-domain recognition mechanism for sialylated and sulfated glycans. *Journal of Biological Chemistry* **2011**, *286* (13), 11346-11355.

19. Bohari, M. H.; Yu, X.; Kishor, C.; Patel, B.; Go, R. M.; Eslampanah Seyedi, H. A.; Vinik, Y.; Grice, I. D.; Zick, Y.; Blanchard, H. Structure-based design of a monosaccharide ligand targeting galectin-8. *ChemMedChem* **2018**, *13* (16), 1664-1672.

20. Costi, R.; Métifiot, M.; Chung, S.; Cuzzucoli Crucitti, G.; Maddali, K.; Pescatori, L.; Messore, A.; Madia, V. N.; Pupo, G.; Scipione, L.; Tortorella, S.; Di Leva, F. S.; Cosconati, S.; Marinelli, L.; Novellino, E.; Le Grice, S. F. J.; Corona, A.; Pommier, Y.; Marchand, C.; Di Santo, R. Basic quinolinonyl diketo acid derivatives as inhibitors of HIV integrase and their activity against RNase H function of reverse transcriptase. *Journal of Medicinal Chemistry* **2014**, *57* (8), 3223-3234.

21. Huang, M.; Grant, G. H.; Richards, W. G. Binding modes of diketo-acid inhibitors of HIV-1 integrase: A comparative molecular dynamics simulation study. *Journal of Molecular Graphics & Modelling* **2011**, *29* (7), 956-964.

22. Corona, A.; Di Leva, F. S.; Thierry, S.; Pescatori, L.; Cuzzucoli Crucitti, G.; Subra, F.; Delelis, O.; Esposito, F.; Rigogliuso, G.; Costi, R.; Cosconati, S.; Novellino, E.; Di Santo, R.; Tramontano, E. Identification of highly conserved residues involved in inhibition of HIV-1 RNase H function by diketo acid derivatives. *Antimicrobial Agents and Chemotherapy* **2014**, *58* (10), 6101-6110.

23. Weidlich, I. E.; Filippov, I. V.; Brown, J.; Kaushik-Basu, N.; Krishnan, R.; Nicklaus, M. C.; Thorpe, I. F. Inhibitors for the hepatitis C virus RNA polymerase explored by SAR with advanced machine learning methods. *Bioorganic & medicinal chemistry* **2013**, *21* (11), 3127-3137.

24. Krieger, I. V.; Freundlich, J. S.; Gawandi, V. B.; Roberts, J. P.; Gawandi, V. B.; Sun, Q.; Owen, J. L.; Fraile, M. T.; Huss, S. I.; Lavandera, J.-L.; Ioerger, T. R.; Sacchettini, J. C. Structure-guided discovery of phenyl diketo-acids as potent inhibitors of M. tuberculosis malate synthase. *Chemistry & biology* **2012**, *19* (12), 1556-1567.

25. Lu, H.; Su, H.; Yang, B.; You, Q.-D. Design, synthesis, and biological activities of histone deacetylase inhibitors with diketo ester as zinc binding group. *Yao Xue Xue Bao* **2011**, *46* (3), 293-298.

26. Hirata, Y.; Sasaki, T.; Kanki, H.; Choong, C.-J.; Nishiyama, K.; Kubo, G.; Hotei, A.; Taniguchi, M.; Mochizuki, H.; Uesato, S. New 5-aryl-substituted 2-aminobenzamide-type HDAC Inhibitors with a diketopiperazine group and their ameliorating effects on ischemia-induced neuronal cell death. *Scientific Reports* **2018**, *8* (1), 1400.

27. Junek, H.; Ziegler, E.; Herzog, U.; Kroboth, H. Eine einfache synthese von malonsäure-mono- und -bis-phenylestern1. *Synthesis* **1976**, *1976* (05), 332-334.

28. Wong, C.-H.; Ye, X. S.; Zhang, Z. Assembly of oligosaccharide libraries with a designed building block and an efficient orthogonal protection-deprotection strategy. *Journal of the American Chemical Society* **1998**, *120* (28), 7137-7138.

29. Sridhar, P. R.; Chandrasekaran, S. Propargyloxycarbonyl (Poc) as a protective group for the hydroxyl function in carbohydrate synthesis. *Organic Letters* **2002**, *4* (26), 4731-4733.

30. Carbain, B.; Martin, S. R.; Collins, P. J.; Hitchcock, P. B.; Streicher, H. Galactose-conjugates of the oseltamivir pharmacophore-new tools for the characterization of influenza virus neuraminidases. *Organic & Biomolecular Chemistry* **2009**, *7* (12), 2570-2575.

31. Bulman Page, P. C.; Moore, J. P. G.; Mansfield, I.; McKenzie, M. J.; Bowler, W. B.; Gallagher, J. A. Synthesis of bone-targeted oestrogenic compounds for the inhibition of bone resorption. *Tetrahedron* **2001**, *57* (9), 1837-1847.

32. Levonis, S. M.; Bornaghi, L. F.; Houston, T. A., Selective monoesterification of malonic acid catalyzed by boric acid. *Australian Journal of Chemistry* **2007**, *60* (11), 821-823.

33. Morris, G. M.; Huey, R.; Lindstrom, W.; Sanner, M. F.; Belew, R. K.; Goodsell, D. S.; Olson, A. J. AutoDock4 and AutoDockTools4: automated docking with selective receptor flexibility. *Journal of computational chemistry* **2009**, *30* (16), 2785-2791.

34. Schuttelkopf, A. W.; van Aalten, D. M. PRODRG: a tool for high-throughput crystallography of protein-ligand complexes. *Acta crystallographica. Section D, Biological crystallography* **2004**, *60* (Pt 8), 1355-1363.

35. Trott, O.; Olson, A. J. AutoDock Vina: Improving the speed and accuracy of docking with a new scoring function, efficient optimization, and multithreading. *Journal of computational chemistry* **2010**, *31* (2), 455-461.

36. McNicholas, S.; Potterton, E.; Wilson, K. S.; Noble, M. E. M. Presenting your structures: the CCP4mg molecular-graphics software. *Acta Crystallographica Section D* **2011**, *67* (4), 386-394.

37. Bohari, M. H.; Yu, X.; Zick, Y.; Blanchard, H. Structure-based rationale for differential recognition of lacto- and neolacto- series glycosphingolipids by the *N*-terminal domain of human galectin-8. *Scientific Reports* **2016**, *6*, 39556.

38. McPhillips, T. M.; McPhillips, S. E.; Chiu, H.-J.; Cohen, A. E.; Deacon, A. M.; Ellis, P. J.; Garman, E.; Gonzalez, A.; Sauter, N. K.; Phizackerley, R. P.; Soltis, S. M.; Kuhn, P. Blu-Ice and the Distributed Control System: software for data acquisition and instrument control at macromolecular crystallography beamlines. *Journal of Synchrotron Radiation* **2002**, *9* (6), 401-406.

39. Kabsch, W. XDS. *Acta Crystallographica Section D* **2010**, *66* (2), 125-132.

40. Evans, P. R.; Murshudov, G. N. How good are my data and what is the resolution? *Acta Crystallographica Section D* **2013**, *69* (7), 1204-1214.

41. Vagin, A.; Teplyakov, A. MOLREP: an automated program for molecular replacement. *Journal of Applied Crystallography* **1997**, *30* (6), 1022-1025.

42. Collaborative, The CCP4 suite: programs for protein crystallography. *Acta Crystallographica Section D* **1994**, *50* (5), 760-763.

43. Murshudov, G. N.; Skubak, P.; Lebedev, A. A.; Pannu, N. S.; Steiner, R. A.; Nicholls, R. A.; Winn, M. D.; Long, F.; Vagin, A. A. REFMAC5 for the refinement of macromolecular crystal structures. *Acta Crystallographica Section D* **2011**, *67* (4), 355-367.

44. Emsley, P.; Lohkamp, B.; Scott, W. G.; Cowtan, K. Features and development of Coot. *Acta Crystallographica Section D* **2010**, *66* (4), 486-501.

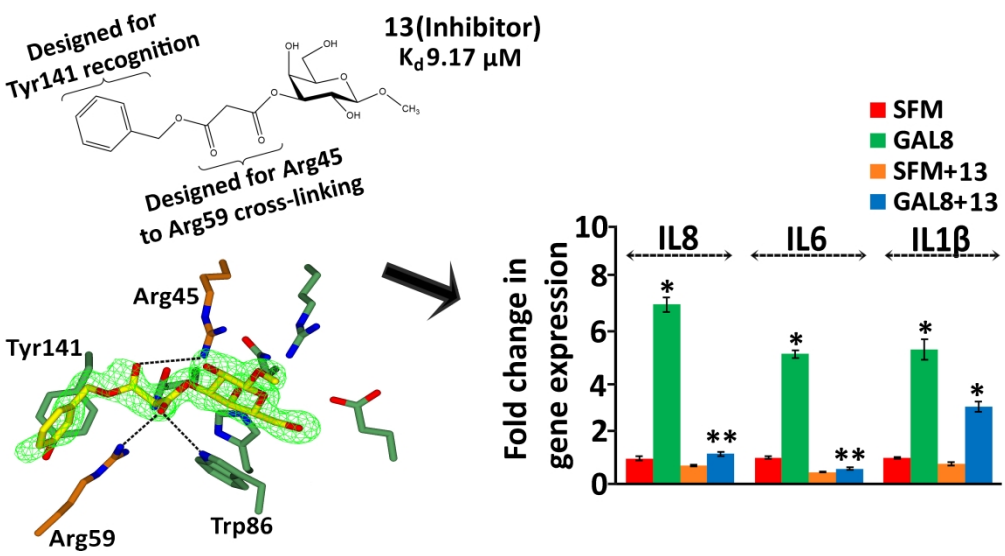

Structure based drug design led to development of monosaccharide galactose based compounds with micro molar binding affinity and moderate to high inhibition of galectin-8 induced cytokines, chemokines expression, making them potent galectin-8 antagonists

82x44mm (1524 x 1524 DPI)